ARTICLES

Ag^+-Inserted NbO_2F as a Novel Photocatalyst

Takashi Murase, Hiroshi Irie, and Kazuhito Hashimoto*

Research Center for Advanced Science and Technology, The University of Tokyo, 4-6-1 Komaba, Meguro-ku, Tokyo 153-8904, Japan

Received: January 24, 2005; In Final Form: May 25, 2005

The insertion of Ag^+ into NbO_2F narrowed the band gap from 3.2 eV (NbO_2F) to 3.0 eV ($Ag-NbO_2F$), which shifted the light absorption edge from the UV light region to the near-violet light region. The photocatalytic activities of NbO_2F and $Ag-NbO_2F$ were evaluated by the decomposition of gaseous 2-propanol (IPA) under 400−530 and 300−400 nm light irradiations. $Ag-NbO_2F$ could decompose IPA to CO_2 via acetone under both irradiation conditions. The value of the quantum efficiency was of the same order under both 400−530 and 300−400 nm light irradiations, which suggested the complete hybridization of the Ag4d and O2p orbitals in the valence band of $Ag-NbO_2F$ resulted in the 400−530 nm light sensitivity. The density of states calculations also supported the complete mixing of Ag4d and O2p.

Introduction

Visible (vis) light sensitive photocatalysts are required to effectively use solar energy and for indoor applications. Numerous studies have reported the sensitization to vis light with respect to TiO_2-based photocatalysts,[1−9] but with the exception of TiO_2-based materials, only a few reports have examined oxide or oxyfluoride materials that are sensitive to vis light for the oxidative decomposition of organic compounds.[10]

NbO_2F,[11] which is in a series of oxyfluorides along with $TiOF_2$,[12] is an electrochromic material with a wide band gap of 3.2 eV.[14−18] This series of oxyfluorides has a simple cubic ReO_3 structure that is a simple cubic ABO_3 perovskite structure where the A site is vacant. NbO_2F is also more stable than $TiOF_2$.[13] However, the photocatalytic properties of NbO_2F have yet to be reported. We are interested in the photocatalytic activity of NbO_2F, but it only responds to UV light since NbO_2F and $SrTiO_3$ have related crystal structures. Also, we expect NbO_2F to be a high-performance photocatalytic material, similar to $SrTiO_3$, which to the best of our knowledge shows a photocatalytic activity as high as TiO_2.[19,20]

As previously mentioned, NbO_2F can absorb only UV light. To effectively use light energy, it is important for NbO_2F to absorb vis light and show photocatalytic activity.

Substituting a cation or anion site in UV light sensitive photocatalysts by a foreign element is a general method for preparing vis light sensitive photocatalysts, such as chromium-doped TiO_2 ($Ti_{1-x}Cr_xO_2$)[21] and nitrogen-doped TiO_2 ($TiO_{2-x}N_x$).[4] Here, we selected Ag^+ as the foreign element and a vacant A site as the insertion site for the following reasons. An ABO_3 perovskite-structured $AgNbO_3$ was reported as a vis light sensitive photocatalyst that possesses the ability to evolve H_2 or O_2 from water in the presence of sacrificial reagents.[22] Vis light absorption of this material is attributed to the hybrid of the Ag4d and O2p orbitals in the valence band, which shifts the top of the valence band to a more negative potential.[22] Since the A site in NbO_2F is vacant and can hold Ag^+, we expect the band gap of NbO_2F to narrow and that NbO_2F could absorb vis light when Ag^+ is inserted into the interstitial site (A site) of NbO_2F.

In the present study, we prepared NbO_2F and Ag^+-inserted NbO_2F (hereafter $Ag-NbO_2F$), and evaluated the photocatalytic oxidation activity by decomposing gaseous 2-propanol (IPA) under light irradiations with wavelengths between 300 and 400 nm and betweem 400 and 530 nm. The correlations between the electronic structures and the photocatalytic properties of NbO_2F and $Ag-NbO_2F$ are discussed.

Experimental Section

NbO_2F powders were prepared by dissolving Nb_2O_5 (Wako Chemical, 99.9%) or Nb (Kojundo Chemical, 99.9%) metal powders in aqueous HF (48%) and subsequently evaporating the excess liquid until dry. The precipitated powders were washed with distilled water, dried under reduced pressure, and then sintered in air at 500 °C for 1 h. $Ag-NbO_2F$ powders were prepared by the conventional solid-state reaction with NbO_2F and Ag_2O powders using the following procedure. NbO_2F and Ag_2O (Wako Chemical, 99%) were thoroughly mixed in a molar ratio of 8:1 and pressed into pellets. The pellets were reacted in air at 500 °C for 10 h, which resulted in $Ag-NbO_2F$.

The crystal phases of the prepared samples were identified by X-ray diffraction (XRD; Rigaku, RINT-2100). The compositions of the samples were determined by X-ray photoelectron spectroscopy (XPS; Perkin-Elmer, 5600). UV−vis absorption spectra using the diffuse reflection method were obtained with a Shimadzu UV-3100 spectrometer. BET surface areas of NbO_2F and $Ag-NbO_2F$ were determined using a nitrogen adsorption apparatus (Micromeritics, TriStar 3000). Grain sizes of the NbO_2F and $Ag-NbO_2F$ powders were observed by scanning electron microscopy (SEM; S-4200, Hitachi Ltd.).

* To whom correspondence should be addressed. Phone: +81-3-5452-5080. Fax: +81-3-5452-6593. E-mail: hashimoto@light.t.u-tokyo.ac.jp.

10.1021/jp050423t CCC: $30.25
Published on Web 06/24/2005

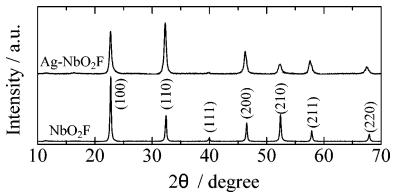

Figure 1. X-ray powder diffraction patterns of NbO_2F and $Ag-NbO_2F$.

The photocatalytic oxidation activity was evaluated by the decomposition of gaseous IPA under light irradiations with wavelengths between 300 and 400 nm and between 400 and 530 nm. Wavelengths of 300−400 and 400−530 nm were achieved using a Xe lamp (Hayashi Tokei, Luminar Ace 210) with a glass filter (Asahi-Technoglass, UV-D36B) and a combination of glass filters (Asahi-Technoglass, B-47, L-42, and C-40C), respectively. The light intensities were 1.0 and 3.0 $mW \cdot cm^{-2}$ for wavelengths between 300 and 400 nm and between 400 and 530 nm, respectively.

A 300 mg sample (NbO_2F or $Ag-NbO_2F$) was evenly spread over the irradiation area (approximately 9.1 cm^2) in a 500 mL vessel. After the sample was sealed in the vessel, the atmosphere in it was replaced by the synthetic air. A 300 ppm (300 ppmv, that is, 6.7 μmol) concentration of reactant gas (IPA) was injected into the vessel, and then the samples were stored in the dark. After confirmation that the IPA concentration was constant, which implied that the reactant gas finished adsorbing onto the powder surface, light irradiation commenced. The photocatalytic oxidation of IPA proceeds via acetone as an intermediate, followed by the slow oxidation of acetone to the final products, CO_2 and H_2O.[23] To evaluate the photocatalytic activity, the amounts of IPA, acetone, and CO_2 were monitored using gas chromatography (Shimadzu, GC-8A).

The plane-wave-based density functional method calculation was carried out for NbO_2F and $Ag-NbO_2F$ within the generalized gradient approximation using the ab initio total energy and molecular dynamics program VASP (Vienna *Ab initio* Simulation Program). The core orbitals were replaced by ultrasoft pseudopotentials, and the kinetic energy cutoff was 500 eV. Actually, the oxygen and fluorine atoms in NbO_2F are randomly distributed. However, to make the calculation easier, the fluorine atoms were placed in trans positions to each other in the calculation of NbO_2F. The composition of $Ag-NbO_2F$ used for the calculation was $Ag_{0.25}NbO_{2.25}F_{0.75}$, which simulated that one-quarter of the NbO_2F interstitial sites are occupied by Ag and that oxygen or fluorine vacancies were not generated.

Results and Discussion

NbO_2F and $Ag-NbO_2F$ were obtained as white and pale yellow powders, respectively. Figure 1 shows the XRD patterns of the obtained samples. The crystal structure of NbO_2F was cubic (*Pm*3*m*, $a = 0.3902$ nm)[13] with a homogeneous crystalline phase. A remarkable change in the peak intensity ratio was observed after insertion of Ag^+ into NbO_2F. The peak intensity of the (110) plane was the strongest in $Ag-NbO_2F$, but the peak intensity of the (100) plane was strongest in NbO_2F. The (110) plane contained the interstitial site in NbO_2F, while the (100) plane did not. Peaks assigned to the Ag atom were not observed. Accordingly, the strongest peak of (110) in $Ag-NbO_2F$ indicated that Ag^+ was inserted into the interstitial site in NbO_2F. The XRD peak positions of $Ag-NbO_2F$ shifted to a lower angle and were accompanied by Ag^+ insertion. Judging from the XRD pattern, $Ag-NbO_2F$ maintained the simple cubic structure. Thus, the cell parameter (*a*) was calculated to be 0.3918 nm.

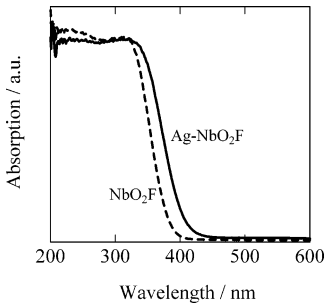

Figure 2. UV−vis absorption spectra of NbO_2F and $Ag-NbO_2F$.

XPS analysis disclosed that the composition of "NbO_2F" was $NbO_{2.02}F_{0.97}$, indicating that the prepared NbO_2F was stoichiometric despite the relatively high annealing temperature (500 °C). XPS confirmed that Ag was introduced as the Ag^+ ion in $Ag-NbO_2F$ and that the composition of $Ag-NbO_2F$ was $Ag_{0.25}NbO_{2.45}F_{0.35}$.[24] Charge balance in $Ag-NbO_2F$ was maintained by fluorine (F^-) elimination and oxygen (O^{2-}) addition, and niobium (Nb^{5+}) was not reduced by Ag^+ insertion. The crystal structure of the obtained $Ag-NbO_2F$ was the one where Ag^+ occupied a quarter of the interstitial sites in the NbO_2F lattice.

The surface areas of NbO_2F and $Ag-NbO_2F$ were determined to be 1.78 and 2.67 $m^2 \cdot g^{-1}$, respectively. According to SEM observations of them, both were agglomerated and had identical powder sizes, 300−1000 nm. Considering Scherrer's equation, the grain sizes of NbO_2F and $Ag-NbO_2F$ were calculated to be 30 and 25 nm, respectively.

Figure 2 shows the UV−vis absorption spectra of NbO_2F and $Ag-NbO_2F$. It was obvious that inserting Ag^+ into NbO_2F narrowed the band gap of $Ag-NbO_2F$. The band gap of $Ag-NbO_2F$ was estimated to be 3.0 eV, which implied that $Ag-NbO_2F$ absorbs light in a longer wavelength region, near-violet light.

The photocatalytic activity of $Ag-NbO_2F$ was compared to that of NbO_2F to determine if $Ag-NbO_2F$ is sensitive to near-violet light (Figure 3a) since the glass filters cannot completely cut off UV light. The light intensity with a wavelength of 400−530 nm was the same for each sample, 3.0 $mW \cdot cm^{-2}$. NbO_2F scarcely showed photocatalytic activity under 400−530 nm light irradiation since it did not absorb 400−530 nm light. However, $Ag-NbO_2F$ showed high activity.[25] Under this condition, $AgNbO_2F$ absorbed a photon flux of 3.7×10^{14} quanta$\cdot cm^{-2} \cdot s^{-1}$. It was assumed that $Ag-NbO_2F$ could completely decompose the injected IPA photocatalytically to the final product, CO_2, since both acetone and CO_2 were produced and the acetone concentration decreased (not shown here) when irradiation was done with 400−530 nm light. The QE value of $Ag-NbO_2F$ under 400−530 nm light irradiation was 0.27%.[26]

IPA decomposition under light irradiation with wavelengths between 300 and 400 nm (1.0 $mW \cdot cm^{-2}$) was also conducted for $Ag-NbO_2F$ and NbO_2F (Figure 3b), which absorbed a photon flux of 1.5×10^{15} and 1.1×10^{15} quanta$\cdot cm^{-2} \cdot s^{-1}$, respectively. As for acetone generation, both $Ag-NbO_2F$ and NbO_2F displayed almost the same photocatalytic activity. However, the photocatalytic activity of NbO_2F was superior to that of $Ag-NbO_2F$ for generating CO_2. The reason will be discussed later. The QE values for NbO_2F and $Ag-NbO_2F$ under 300−400 nm light irradiation were 0.21% and 0.14%, respectively. The observation of smaller QE (0.14%, compared to 0.27%) for irradiation with 300−400 nm light in the presence of $Ag-NbO_2F$ should originate from the larger absorbed photon number of 1.5×10^{15} quanta$\cdot cm^{-2} \cdot s^{-1}$, compared to that of

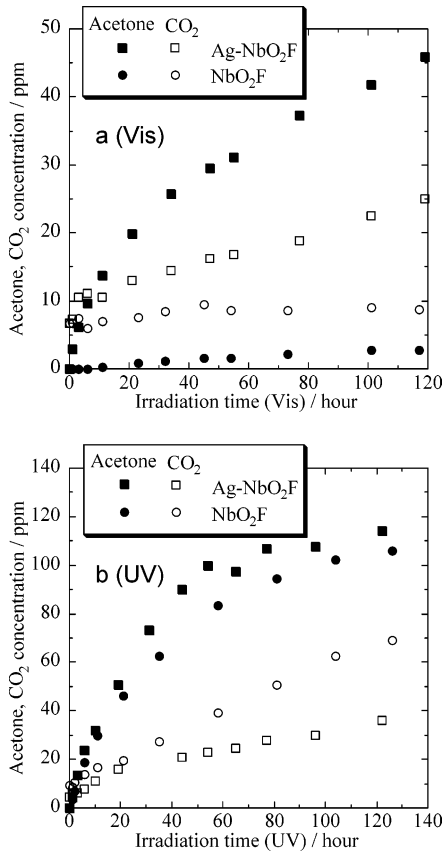

Figure 3. Changes in acetone and CO_2 concentrations by IPA decomposition as a function of time in the presence of Ag−NbO_2F or NbO_2F under (a) light with wavelengths between 400 and 530 nm (3.0 mW·cm^{-2}) and (b) light with wavelengths between 300 and 400 nm (1.0 mW·cm^{-2}).

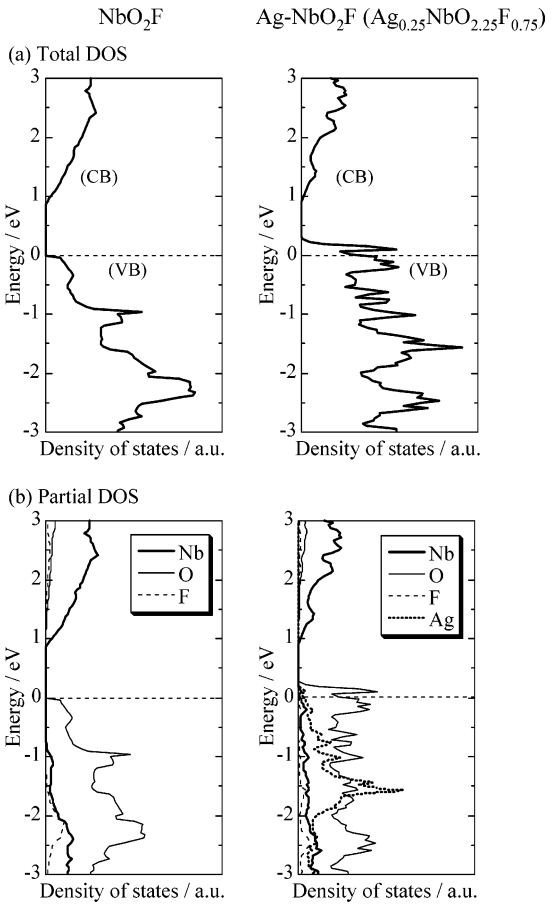

Figure 4. Total (a) and partial (b) densities of states for NbO_2F (left) and Ag−NbO_2F (right). The energy was measured from the top of the valence band in NbO_2F (the horizontal dashed line). The composition of Ag−NbO_2F for the calculation was $Ag_{0.25}NbO_{2.25}F_{0.75}$.

3.7×10^{14} quanta·cm^{-2}·s^{-1} under 400−530 nm light. So it can be suggested that those QE values are essentially similar in both wavelength ranges. The composition of Ag−NbO_2F after 300−400 nm light irradiation for 150 h with an intensity of 1.0 mW/cm^2 was almost constant, $Ag_{0.25}NbO_{2.54}F_{0.34}$, within the experimental error determined by XPS. Thus, Ag−NbO_2F is a stable photocatalyst.

The electronic structures of NbO_2F and Ag−NbO_2F were calculated to ensure that inserting Ag^+ into the interstitial site of NbO_2F decreased the band gap. Figure 4 shows the density of states (DOS) of NbO_2F and Ag−NbO_2F. It was determined that the fluorine orbitals contributed to neither the valence nor conduction band due to its large electronegativity. The orbitals of silver did not contribute to the conduction band in Ag−NbO_2F. Therefore, the bottom of the conduction band in Ag−NbO_2F was the same level as that in NbO_2F. The valence band in Ag−NbO_2F consisted of the Ag4d and O2p hybrid orbitals, and the top of the valence band shifted to the high-energy side, which decreased the band gap energy. Hence, the DOS calculations and UV−vis absorption spectrum confirmed that Ag is a promising element for narrowing the band gap of oxides and oxyfluorides.

As mentioned in Figure 4, the top of the valence band in Ag−NbO_2F shifted to the high-energy side compared to that of NbO_2F due to the hybridization of the Ag4d and O2p orbitals. The position of the top of the valence band determines the oxidation power of a photogenerated hole, and its activity increases as the top of the valence band shifts to the low-energy side. Therefore, the oxidation power of the hole generated in Ag−NbO_2F is weaker than that in NbO_2F. The oxidative decomposition of IPA to acetone proceeds easily, but a strong oxidation power is necessary for the complete oxidative decomposition of acetone to CO_2. Therefore, under 300−400 nm light irradiation, it is plausible that the oxidative decomposition of IPA to acetone is comparable in the presence of Ag−NbO_2F and NbO_2F, but the complete oxidative decomposition of acetone to CO_2 by Ag−NbO_2F is relatively slow.

The QE values of Ag−NbO_2F under 400−530 and 300−400 nm light irradiations indicated that the photocatalytic activity is similar in both wavelength ranges. This tendency strongly implies that the Ag4d and O2p orbitals completely mix to form the valence band of Ag−NbO_2F, which is consistent with the calculated DOS of Ag−NbO_2F. The reasons are as follows. As soon as the free charge carriers are photogenerated in a semiconductor, such as TiO_2, and there is rapid communication between the valence band and conduction band, the photocarriers will occupy the lowest states in their corresponding bands (i.e., they become thermalized). The carrier temperature becomes equal to ambient temperature, and the carriers are indistinguishable regardless of the initial state immediately occupied upon photoexcitation. That is, the excess photoenergy is dissipated as heat rather than as chemical potential.

Conclusion

NbO_2F was successfully improved to absorb near-violet light by inserting Ag^+ into the interstitial site of the NbO_2F lattice. Ag−NbO_2F showed photocatalytic activity under near-violet light irradiation (400−530 nm). The photocatalytic activities of Ag−NbO_2F under 300−400 and 400−530 nm light irradia-

tions were of the same order, which is due to the complete mixing of the Ag4d and O2p orbitals in the valence band of $Ag-NbO_2F$.

The present study demonstrated that introducing Ag^+ into oxides or oxyfluorides that are sensitive to UV light is a potential approach for generating photocatalysts that are sensitive to near-violet light. Herein, introducing Ag^+ into NbO_2F narrowed the band gap only from 3.2 to 3.0 eV, probably due to the low Ag^+ concentration. However, we believe that introducing more Ag^+ into NbO_2F may prepare vis light sensitive $Ag-NbO_2F$. Further investigations are currently under way.

Acknowledgment. This work was supported by a Grant-in-Aid for Scientific Research on Priority Areas (417) from the Ministry of Education, Culture, Sports, Science and Technology (MEXT) of the Japanese Government.

References and Notes

(1) Borgarello, E.; Kiwi, J.; Grätzel, M.; Pelizzetti, E.; Visca, M. *J. Am. Chem. Soc.* **1982**, *104*, 2996.

(2) Yamashita, H.; Ichihashi, Y.; Takeuchi, M.; Kishiguchi, S.; Anpo, M. *J. Synchrotron Radiat.* **1999**, *6*, 451.

(3) Anpo, M.; Takeuchi, M. *Int. J. Photoenergy* **2001**, *3*, 1.

(4) Asahi, R.; Morikawa, T.; Ohwaki, T.; Aoki, K.; Taga, Y. *Science* **2001**, *293*, 269.

(5) Khan, S. U. M.; Al-Shahry, M.; Ingler, W. B., Jr. *Science* **2002**, *297*, 2243.

(6) Umebayashi, T.; Yamaki, T.; Tanaka, S.; Asai, K. *Chem. Lett.* **2003**, *32*, 330.

(7) Ohno, T.; Mitsui, T.; Matsumura, M. *Chem. Lett.* **2003**, *364*, 330.

(8) Irie, H.; Watanabe, Y.; Hashimoto, K. *J. Phys. Chem. B* **2003**, *107*, 5483.

(9) Irie, H.; Washizuka, S.; Yoshino, N.; Hashimoto, K. *Chem. Commun.* **2003**, *11*, 1298.

(10) Miyauchi, M.; Takashio, M.; Tobimatsu, H. *Langmuir* **2004**, *20*, 232.

(11) Frevel, L. K.; Rinn, H. W. *Acta Crystallogr.* **1956**, *9*, 626.

(12) Vorres, K. S.; Dutton, F. B. *J. Am. Chem. Soc.* **1955**, *77*, 2019.

(13) Grannec, J.; Yacoubi, A.; Ravez, J.; Hagenmuller, P. *J. Solid State Chem.* **1988**, *75*, 263.

(14) Murphy, D. W.; Greenblatt, M.; Cava, R. J.; Zahurak, S. M. *Solid State Ionics* **1981**, *5*, 327.

(15) Permér, L.; Lundberg, M. *J. Solid State Chem.* **1989**, *81*, 21.

(16) Permér, L.; Lundberg, M. *J. Less-Common Met.* **1989**, *156*, 145.

(17) Bohnke, C.; Fourquet, J. L.; Randrianantoandro, N.; Brousse, T.; Crosnier, O. *J. Solid State Electrochem.* **2001**, *5*, 1.

(18) Mizoguchi, H.; Orita, M.; Hirano, M.; Fujitsu, S.; Takeuchi, T.; Hosono, H. *Appl. Phys. Lett.* **2002**, *80*, 4732.

(19) Miyauchi, M.; Nakajima, A.; Fujishima, A.; Hashimoto, K. Watanabe, T. *Chem. Mater.* **2000**, *12*, 3.

(20) Miyauchi, M.; Nakajima, A.; Watanabe, T.; Hashimoto, K. *Chem. Mater.* **2002**, *14*, 2815.

(21) Anpo, M. *Catal. Surv. Jpn.* **1997**, *1*, 169.

(22) Kato, H.; Kobayashi, H.; Kudo, A. *J. Phys. Chem. B* **2002**, *106*, 12441.

(23) Larson, S. A.; Widegren, J. A.; Falconer, J. L. *J. Catal.* **1995**, *157*, 611.

(24) Waring, J. L.; Roth, R. S.; Parker, H. S. *J. Res. Natl. Bur. Stand., Sect. A* **1973**, *77*, 705.

(25) In fact, we have not observed the complete decomposition of the injected IPA to CO_2. The decrease of IPA did not balance with the increase of acetone and CO_2 for the following reason. IPA is easily decomposed to acetone, but acetone is decomposed to CO_2 with difficulty, and some substrate remains as intermediates during the acetone decomposition to CO_2. This phenomenon was also observed in the presence of TiO_2 irradiated even with UV light before the complete decomposition of IPA to CO_2 was finished.

(26) The quantum efficiency (QE; the same as photonic efficiency) calculations were conducted using the same procedure as Murase, T.; Irie, H.; Hashimoto, K. *J. Phys. Chem. B* **2004**, *108*, 15803. The initial acetone and CO_2 generation rates by IPA decomposition were calculated using the conventional least-squares method. Only one photon participates in the decomposition process of IPA to acetone. Therefore, the QE values for acetone generation were calculated using the following equation: $QE_{acetone}$ = (initial acetone generation rate)/(absorption rate of incident photons). For example, the absorbed photon number was 3.7×10^{14} quanta·cm^{-2}·s^{-1} for $Ag-NbO_2F$ irradiated with 400−530 nm light. Hence, the absorption rate of the incident photons was 3.4×10^{15} quanta·s^{-1} ($(9.1\ cm^2)(3.7 \times 10^{14}$ quanta·cm^{-2}·$s^{-1}) = 3.4 \times 10^{15}$ quanta·s^{-1}). The initial acetone generation rate was 7.4×10^{-12} mol·s^{-1}. Thus, $QE_{acetone} = [(7.4 \times 10^{-12}$ mol·$s^{-1})(6.0 \times 10^{23}$ quanta·$mol^{-1})]/$(3.4 \times 10^{15}$ quanta·$s^{-1}) = 1.4 \times 10^{-3}$ (=0.14%). Compared to the mechanism for acetone generation, the mechanism for CO_2 generation is complex. Thus, it is difficult to determine the number of photons participating in the reaction since there are two reaction paths. Assuming the formula $C_3H_8O + 5H_2O + 18h^+ \rightarrow 3CO_2 + 18H^+$, that is, six photons are required to produce one CO_2 molecule, the QE values for CO_2 generation were calculated using the following equation: QE_{CO_2} = 6(initial CO_2 generation rate)/(absorption rate of incident photons). That is, $QE_{CO_2} = [6(1.2 \times 10^{-12}$ mol·$s^{-1})(6.0 \times 10^{23}$ quanta·$mol^{-1})]/$(3.4 \times 10^{15}$ quanta·$s^{-1}) = 1.3 \times 10^{-3}$ (=0.13%). Thus, the apparent total QE value = $QE_{acetone} + QE_{CO_2}$ = 0.14% + 0.13% = 0.27%.